Hydrogeol J (2017) 25:829–845
DOI 10.1007/s10040-016-1513-9

PAPER

Interlobate esker architecture and related hydrogeological features derived from a combination of high-resolution reflection seismics and refraction tomography, Virttaankangas, southwest Finland

Georgiana Maries[1] · Elina Ahokangas[2] · Joni Mäkinen[2] · Antti Pasanen[3] · Alireza Malehmir[1]

Received: 25 April 2016 / Accepted: 4 December 2016 / Published online: 29 December 2016

Abstract A novel high-resolution (2–4 m source and receiver spacing) reflection and refraction seismic survey was carried out for aquifer characterization and to confirm the existing depositional model of the interlobate esker of Virttaankangas, which is part of the Säkylänharju-Virttaankangas glaciofluvial esker-chain complex in southwest Finland. The interlobate esker complex hosting the managed aquifer recharge (MAR) plant is the source of the entire water supply for the city of Turku and its surrounding municipalities. An accurate delineation of the aquifer is therefore critical for long-term MAR planning and sustainable use of the esker resources. Moreover, an additional target was to resolve the poorly known stratigraphy of the 70–100-m-thick glacial deposits overlying a zone of fractured bedrock. Bedrock surface as well as fracture zones were confirmed through combined reflection seismic and refraction tomography results and further validated against existing borehole information. The high-resolution seismic data proved successful in accurately delineating the esker cores and revealing complex stratigraphy from fan lobes to kettle holes, providing valuable information for potential new pumping wells. This study illustrates the potential of geophysical methods for fast and cost-effective esker studies, in particular the digital-based landstreamer and its combination with geophone-based wireless recorders, where the cover sediments are reasonably thick.

Keywords Esker architecture · Landstreamer · Unconsolidated sediments · Geophysical methods · Finland

Electronic supplementary material The online version of this article (doi:10.1007/s10040-016-1513-9) contains supplementary material, which is available to authorized users.

✉ Georgiana Maries
georgiana.maries@geo.uu.se

[1] Department of Earth Sciences, Uppsala University, Uppsala, Sweden

[2] Department of Geography and Geology, University of Turku, Turku, Finland

[3] Unit of Industrial Environments and Recycling, Geological Survey of Finland (GTK), Kuopio, Finland

Introduction

Eskers, defined as stratified sediments of gravel and sand deposited by glacial melt-water streams (Banerjee and McDonald 1975; Shreve 1985; Hebrand and Åmark 1989; Gorrell and Shaw 1991; Warren and Ashley 1994; Huddart et al. 1999; Brennand 2000), are hydrogeological settings of great significance in areas that have undergone glaciation such as in Finland, Sweden, the British Isles, USA and Canada. They are remarkable aquifers that are often used also for construction aggregates, thus an accurate understanding and subsurface delineation of the large-scale structures as well as hydrogeological units within these precious groundwater reservoirs is essential for their environmental and economic usage (Boucher et al. 2015; Nadeau et al. 2015). Eskers host marked groundwater aquifers and sites for managed aquifer recharge (MAR) plants for groundwater production (Artimo et al. 2010; Jokela and Kallio 2015).

Eskers are also associated with tunnel channels (or tunnel valleys) which are the erosive expression of channelized subglacial water flows and often truncate subglacial bedforms and/or till (Burke et al. 2012). A few exceptionally large eskers, like the Säkylänharju-Virttaankangas complex in southwest Finland, are attributed to time-transgressive deposition within an interlobate joint between two differently behaving ice streams (Punkari 1980; Kujansuu et al. 1995; Mäkinen 2003a). Interlobate esker complexes are extensive and are characterized by up to 100-m-thick glacial sediments comprising of large-scale depositional units with a wide range of internal structures. Therefore, these complexes demand deep penetrating investigation methods that can provide a link between bedrock surface topography and large-scale esker elements in order to reliably model hydrogeological units as well as the related groundwater flow.

An efficient way to recharge aquifers for environmental or economic benefits such as providing fresh water supplies for entire communities (Bouwer 2002; Dillon 2005), MAR applications benefit from increasing multidisciplinary studies that combine geophysical methods and hydrogeology aspects (Rossi et al. 2014; Ulusoy et al. 2015). Near-surface geophysical methods have routinely been used for engineering, geotechnical, environmental or hydrogeological applications (Telford et al. 1990; Sheriff and Geldart 1995), but in the last 30 years the high-resolution reflection seismic method, the primary choice for hydrocarbon exploration, has also been employed for near-surface investigations (Steeples and Miller 1988); several case studies attest their effectiveness (Miller et al. 1989; Baker et al. 2000; Juhlin et al. 2002; Pugin et al. 2004a; Schmelzbach et al. 2005; Sloan et al. 2007; Malehmir et al. 2013a, b). Seismic methods (refraction and reflection), like other geophysical methods, are non-invasive and provide an efficient tool for delineating shallow (<150 m) yet heterogeneous, geologically complex targets such as groundwater reservoirs, aquifers and structures hosting or controlling their locations (Pullan et al. 1994; Bradford 2002; Sharpe et al. 2003; Huuse et al. 2003; Francese et al. 2005; Giustiniani et al. 2008; Burke et al. 2008; Pasanen 2009; Comas et al. 2011). There is a gradual shift towards acquiring high-resolution seismic data, in particular within unconsolidated or normally consolidated sediments, by employing fast and cost-effective methods such as seismic landstreamers (van der Veen and Green 1998; van der Veen et al. 2001; Huuse et al. 2003; Pugin et al. 2004a, b, 2009a, b; Almholt et al. 2013).

Continuous developments in the acquisition systems and sensor types have led to landstreamers being employed for numerous near surface investigations, including groundwater and glacial landform studies, proving their time- and cost-effective acquisition with high data quality. By definition, a landstreamer is an array of seismic sensors that can be towed behind a vehicle without the need for planting the sensors (Kruppenbach and Bedenbender 1975). While most landstreamers use geophones (analogue systems) for data acquisition, a newly developed advanced MEMs-based (micro-electro mechanical) broadband seismic landstreamer (Brodic et al. 2015; Malehmir et al. 2015a, 2015b, 2016a, 2016b) was employed in this study for delineating subsurface structures of a major interlobate esker system and a MAR aquifer in Virttaankangas, in the southwest of Finland.

Prior to this study, in 2011, a pilot test of employing a seismic landstreamer was conducted at Virttaankangas using geophones (Pugin et al. 2014) indicating the applicability of the method, but with some uncertainties in separation of bouldery esker deposits, diamictons and bedrock facies. The main objective of this study is to test the applicability of the newly developed MEMs-based landstreamer (Brodic et al. 2015) as an advanced seismic method for aquifer characterization within complex glaciofluvial deposits with thick (10–40 m) dry sediments above the water table. The present study focuses on the coarse-grained glaciofluvial hydrogeological unit that forms the main Virttaankangas esker aquifer (Artimo et al. 2003) within the MAR plant area. The main aquifer includes the boulder-rich esker core (50–150 m wide) that has a high hydraulic conductivity—10^{-4} to 10^{0} m/s for the whole coarse-grained unit (Artimo et al. 2003) and is the target for pumping station locations.

The seismic data were expected: (1) to help locate the high hydraulic conductivity esker core and its stratigraphic position within the fractured bedrock zone, including bedrock overlaying diamictons, (2) to delineate large-scale architectural esker elements (esker core, fan lobe channels) within the coarse-grained hydrogeological unit of the MAR plant, (3) to define large-scale deformation structures (morphologically undetectable kettle holes, MUKHs) and their bedrock contact (influence on MAR residence times and groundwater flow paths), and (4) to characterize the lateral relationships of the esker elements and the underlying bedrock surface. In addition, one of the two seismic profiles, profile 2, was designed to accurately delineate the esker core for locating new pumping stations within the widest and structurally most complicated part of the coarse-grained unit. This is the first case study where an advanced high-resolution seismic landstreamer survey has been utilized for aquifer characterization and validation of the hydrogeological properties within an interlobate esker system. Results illustrate the potential of the combined refraction and reflection methods for these purposes.

Study area

Field area

The Säkylänharju-Virttaankangas (S-V) glaciofluvial complex forms a part of the 150-km-long Koski-Pori esker chain in southwest Finland (Fig. 1). The Virttaankangas plain hosts an operational MAR plant that provides a potable water resource for over 300,000 inhabitants within the Turku city region (Artimo et al. 2003, 2008). The MAR plant consists of several infiltration ponds and pumping stations as well as numerous observation wells at strategic locations within the eskers elements (e.g. Fig. 2) that provide groundwater levels and lithological characterization with bedrock information at

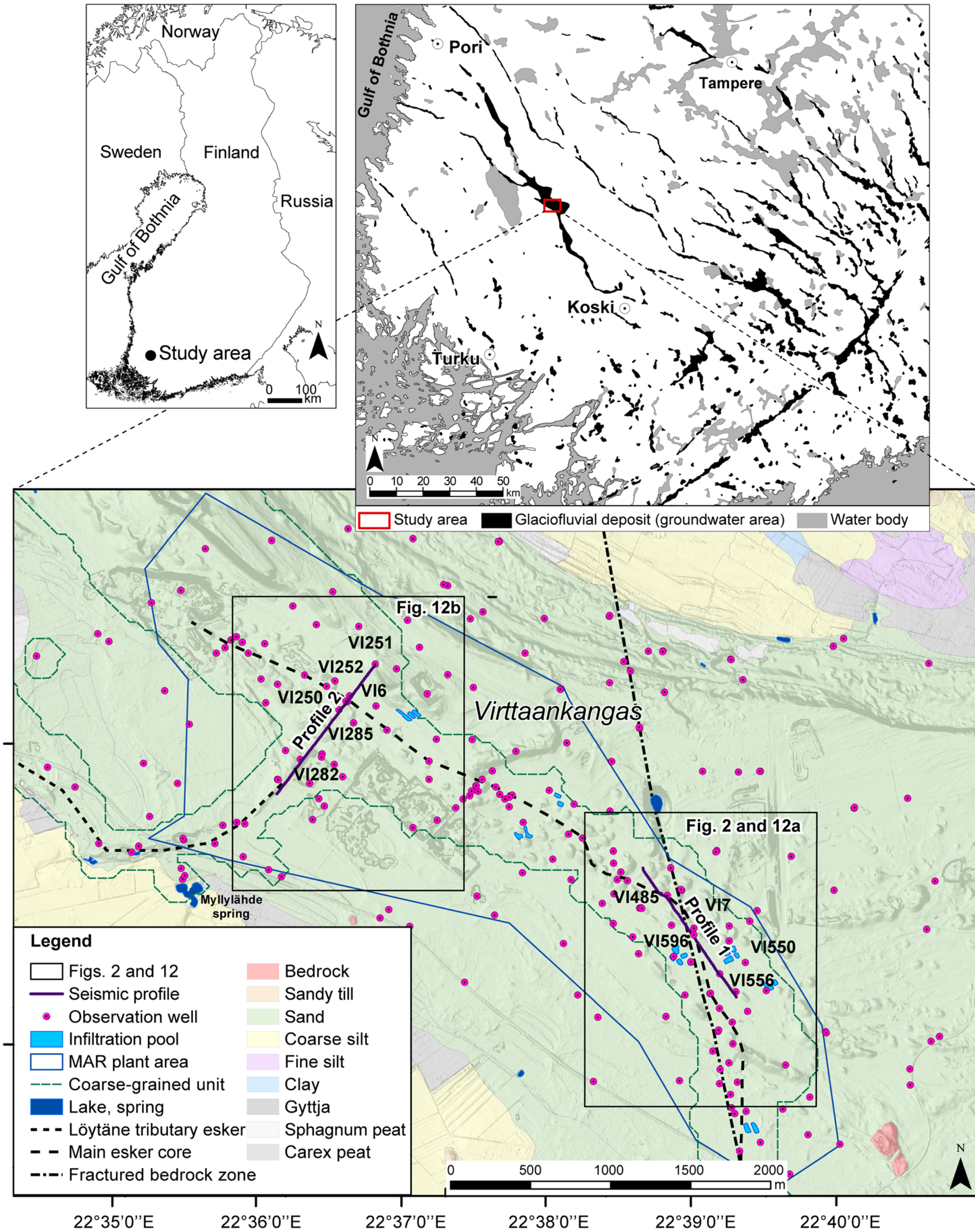

Fig. 1 Virttaankangas study area near the city of Turku and the location of the seismic profiles (profiles 1 and 2), main esker core, Löytäne tributary esker, Myllylähde spring and fractured bedrock zone. The extent of the MAR plant area with infrastructure (observation wells and infiltration pools) and the coarse-grained unit provided by Turku Region Water Ltd. The index map groundwater areas © Finnish Environment Institute (2016), coastline and water bodies © NLS (2016).The map of superficial deposits of Finland © Geological Survey of Finland and the base map and LiDAR © NLS (2010)

scattered locations. A finite-difference (grid-type) groundwater flow model within an area of 80 km^2 includes the description of the geometry of the hydrogeological units (Fig. 3). The flow parameters of the coarse-grained unit studied herein have been described in more detail than within the rest of the model (A. Artimo, Turku Region Water Ltd, personal communication, 2016). The flow model incorporates a depositional model of the esker verified with infiltration and pumping tests as well as tracer tests including oxygen isotopes of infiltrated water. The depositional model is based on extensive ground penetrating radar (GPR) surveys (21 km) supported by reference data from boreholes and exposed gravel/sand pits (Artimo et al. 2010). Bedrock topography is provided by a rough modeling of a network of gravity data points (Valjus 2006). The

Fig. 2 Main esker architecture elements and MAR plant infrastructure in relation to the main bedrock fracture in the vicinity of seismic profile 1 in the eastern part of Virttaankangas. The hydraulic importance of the large-scale cross-bedded fan lobes is depicted by their impact on flow direction of the infiltrated water and related residence times due to the dip of the cross beds as seen in one of the infiltration areas. Bedrock elevation contours modified from Valjus (2006)

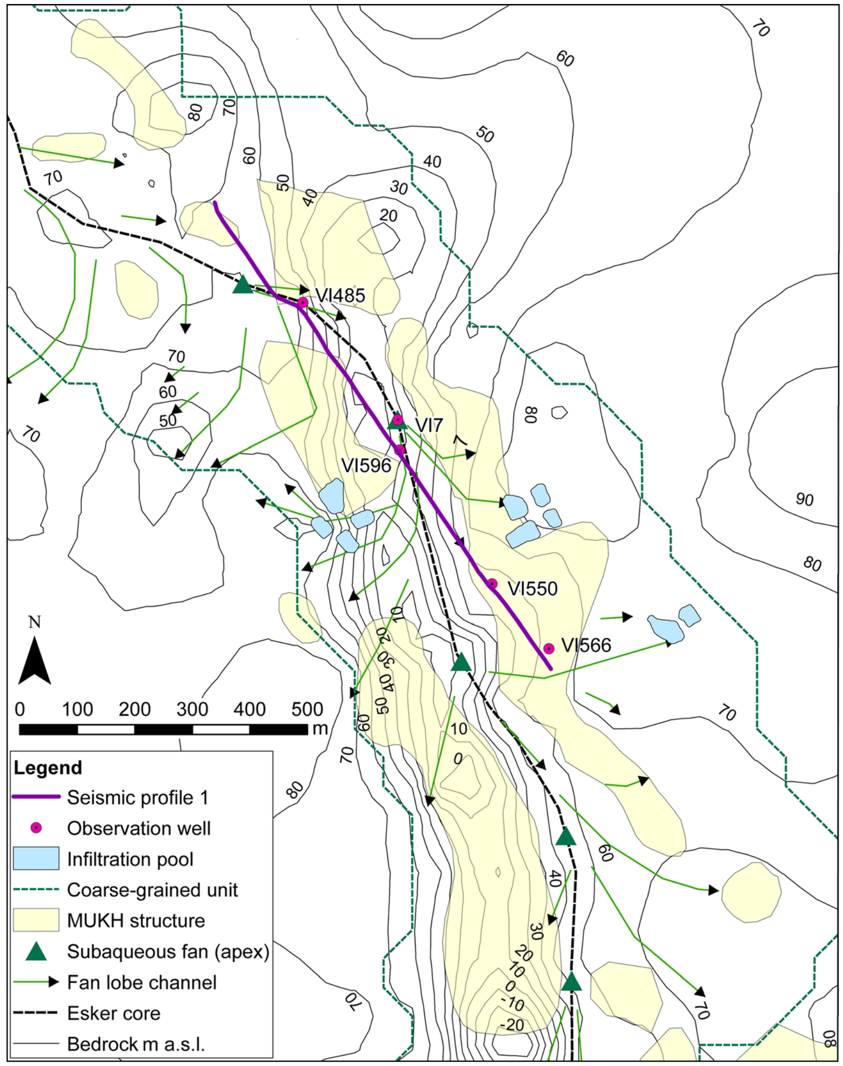

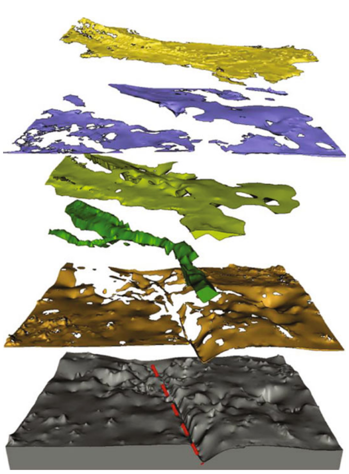

Fig. 3 The main 3-D hydrogeological units of the Virttaankangas aquifer (From: Artimo et al. 2010). The esker core is contained within the glaciofluvial coarse-grained unit. MUKH structures are treated as a separate unit. *Red dashed line* in the bottom unit represents fractured bedrock

depositional environments and related depositional stages during the last deglaciation as well as related main hydrogeological units have been studied earlier by several authors (Artimo et al. 2003; Mäkinen 2003a, b; Mäkinen and Räsänen 2003). The two survey profiles in this study were targeted to delineate the most complex parts of the coarse-grained hydrogeological unit (Fig. 1).

Geological setting and three-dimensional geologic model

The Säkylänharju-Virttaankangas (S-V) glaciofluvial complex is situated on the Precambrian Svecofennian basement of igneous and metamorphic rocks (1,750–1,900 Ma) located 10–15 km southeast of the basement contact with the younger Jotnian Satakunta sandstones (1,200–1,500 Ma; Korsman et al. 1997). The Säkylänharju main ridge is about 1–2 km wide with a summit (Porsaanharju) rising close to the ancient highest shoreline. The main ridge gradually decreases in height into Virttaankangas, a 5 km fan-like plain in the southeast (Fig. 1.) The core of the main esker is connected to the smaller 10–15-m-thick core of the Löytäne tributary esker (aquifer) in the northwestern end of the MAR plant area. The tributary esker sediments route the groundwater flow towards the Myllylähde spring (discharge ca. 2,500 m^3/day) in the southwest side of the glaciofluvial complex. The glaciofluvial sediments have a thickness of 10–40 m, reaching over 70 m in some places. A major fractured bedrock zone of about 200–300 m wide and 45–80 m deep has been inferred at Virttaankangas in NNW–SSE orientation (Fig. 1). The esker core and fan sediments turn to follow the fracture zone towards the south, but the stratigraphy of the zone is not adequately described. A few deep boreholes (e.g. VI596) within the fracture zone display poorly hydraulically conductive diamicton below the esker core.

The Säkylänharju main ridge formed in a large interlobate ice-marginal embayment (as subaqueous crevasse deposits) of the deglacial Yoldia Sea Phase and was altered by intense shoreline erosion during the rapid glacio-isostatic land uplift (Mäkinen 2003a, b). The coarse-grained parts of the main esker ridge have been levelled less by the shore erosion, leading to only 1–3-m-thick littoral sand and gravel deposits in contrast to the surrounding plain. The wide eastern part of the plain, that covers sandy and fine-grained glaciofluvial sediments, is composed of postglacial shore deposits (5–20 m thick) formed during a spit-platform development in the Ancylus Lake phase of the ancient Baltic Sea (Mäkinen and Räsänen 2003).

The internal architecture of the Virttaankangas area includes the coarse-grained and continuous subglacially formed esker core covered by ice-marginally deposited overlapping, successive esker fans (Mäkinen 2003b). These fans show large cross-bedded fan lobe structures, laterally fining and upward coarsening sequences, as well as large-scale deformation often related to MUKH structures (Mäkinen 2003b) that well delineate the path of the esker core (see Fig. 2). Figure 4 shows a conceptual 3D model of the area with simplified geology and internal architecture of the esker elements based on earlier GPR surveys supported with borehole data, sediment exposures and hydrogeological data. However, the GPR data are restricted to the topmost 20 m. Some of the depositional features (fan lobe channels, a MUKH structure and the bouldery esker core) are illustrated through field photos (Fig. 5) from an aggregate pit in the vicinity of the main esker core. MUKH structures were formed when buried blocks of ice melt and subsequently the holes were filled with collapsing esker fan sediments and shore deposits. Especially large MUKH structures beside the esker core have been interpreted to extend down to bedrock (Artimo et al. 2010). Finally, the fan and kettle hole morphology have been levelled by intense erosion (10–20 m) due to shoreline processes. The large MUKH structures with often fine-grained margins have marked influence on groundwater flow properties and are thus treated as separate sedimentological units in the groundwater flow model (Artimo et al. 2003, 2010). Moreover, MUKH structures have been used to create reverse gradients between infiltration ponds and pumping stations. The connection of the Säkylänharju main esker core and Löytäne tributary esker

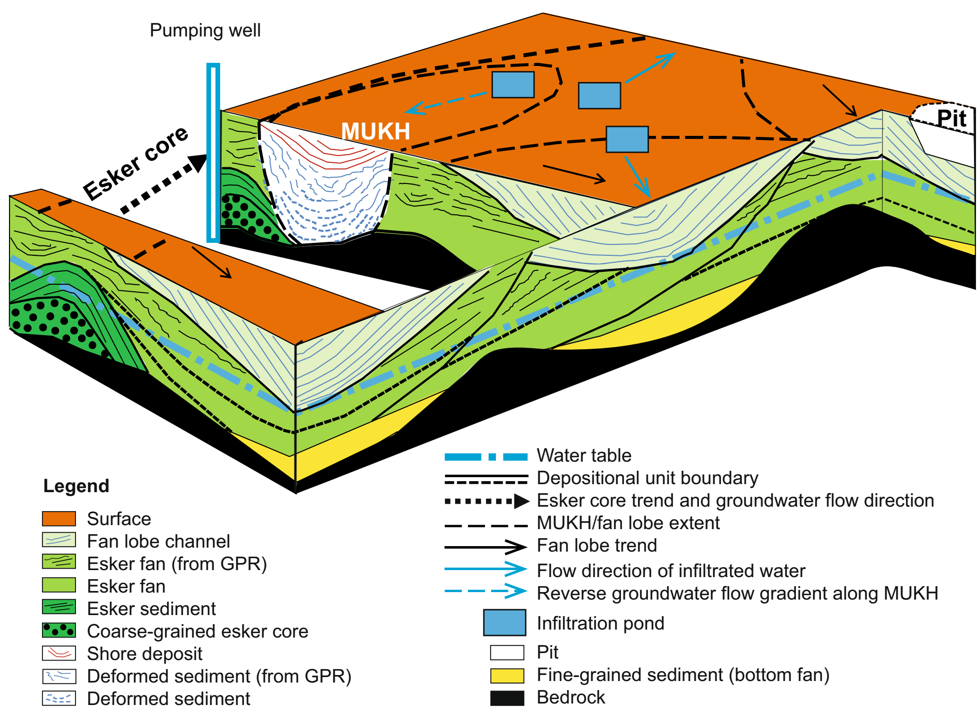

Fig. 4 Schematic model of the successive esker fans and the main depositional and hydrogeological units. *Green color* represents overlapping esker fans with distinct fan lobe channels, while *yellow color* refers to fan bottom fine-grained sediments. MUKH refers to morphologically undetectable kettle hole. The model is based on GPR surveys with reference data from pit exposures and boreholes. The main components of the MAR plant (pumping wells and infiltration ponds) are included with the directions of infiltrated water flow in relation to the main esker elements. Bedrock (*in black*) is based on gravity modelling and boreholes

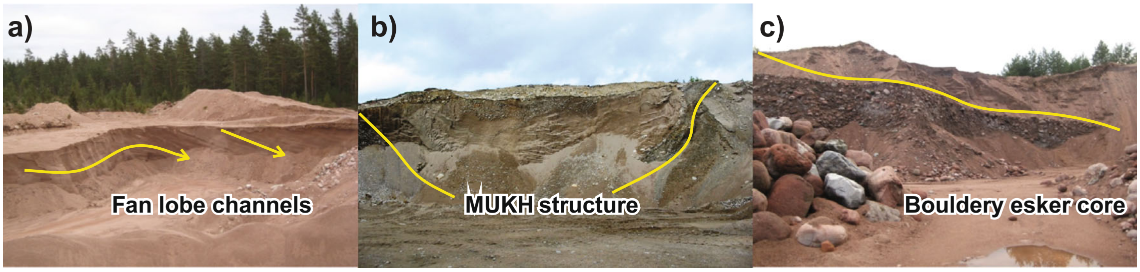

Fig. 5 Field photos from an aggregate pit in the vicinity of the main esker core that show typical elements found in the internal architecture of an esker system; similar landforms to the ones interpreted and discussed later in the paper: **a** fan lobe channels; **b** typical MUKH structure; **c** bouldery esker core. Photos by Elina Ahokangas and Joni Mäkinen

cores is still poorly known, but it forms a marked widening of the coarse-grained hydrogeological unit. This widening is also associated with a secondary esker enlargement on the eastern side of the main core. The proximal part of the enlargement is situated on the main Säkylänharju ridge (ice-marginal crevasse deposits), whereas the distal part is composed of mostly fine-grained sediments below the shore deposits of the Virttaankangas plain (Mäkinen 2003b).

Methods

Seismic data acquisition

The seismic survey consisted of two seismic profiles (profiles 1 and 2), each about 1 km long, in the proximity of the water company infiltration pools (Figs. 1 and 2). Profile 1 was set up along a sandy road, roughly in NW–SE direction (Fig. 2). With a similar set-up, orientated in SW–NE, profile 2 was surveyed on a sandy road, 200 m away from profile 1, next to an old open pit, but continued on a trail in the forest on loose sandy sediments. Figure 6 shows two photos illustrating the data acquisition and field conditions along profile 2. The profile locations were designed to intersect the estimated esker core positions (profiles 1 and 2), to reveal the esker stratigraphy in the fractured bedrock (profile 1), and to illustrate the cross-sectional structure of the main esker aquifer (profile 2).

Sercel Lite 428 data acquisition system and a newly developed 200 m-long landstreamer comprising of 80-3C (three component) MEMs sensors (Brodic et al. 2015) were used for the data acquisition. 3C sensors record the wave motion along three axes, one vertical and two horizontal, where the horizontal components are in-line relative to the sensor array, and cross-line (perpendicular) to the sensor array, respectively; the sensor array is set up in the in-line direction. The array consisted of, at the time of the survey, four segments each containing 20 sensors; in one segment sensors were spaced 4 m apart and in the other three they were spaced at 2 m. Easily towed by a 4 WD vehicle (Fig. 6), the landstreamer array was moved until the desired survey length was covered. In order to account for the low fold at the end points of each segment, 51 single component wireless sensors connected to 10-Hz geophones were deployed along the profiles, spaced at about every 20 m. The landstreamer system and the acquisition unit used to acquire the data use GPS time for time sampling and time stamping; hence, it allows them to be merged at later times with wireless recorders that operate in a passive mode (continuous recording).

The same geometry spread was used for both seismic refraction and reflection data. Seismic energy was generated using a Bobcat-mounted 500-kg drop-hammer (Place et al. 2015), with three shot records per location in order to provide high signal-to-noise ratio after the vertical stacking of the repeated shot records. Given the nature of the source, only the vertical component data were used in the present study. The shot spacing was kept 4 m for both profiles and the energy source proved to be a good choice despite the dry and unconsolidated glacial sediments that can highly attenuate the seismic response. Shallow reflections are identifiable in most shot gathers, implying that the source was optimal for this survey.

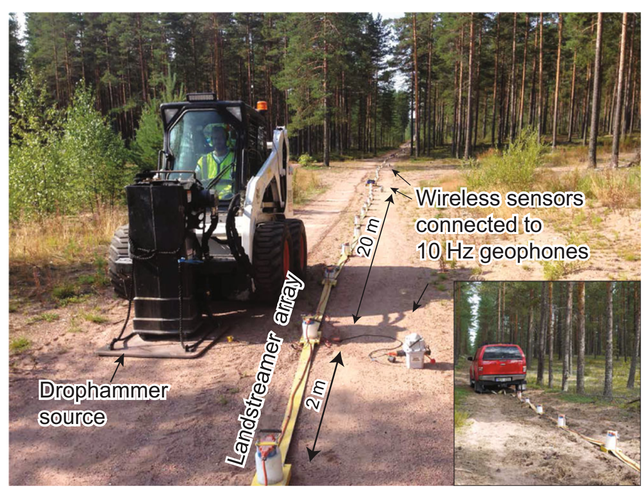

Fig. 6 Field conditions during the seismic survey (July 2014). Bobcat mounted drop-hammer (500 kg) was used to generate seismic energy at every shot location (only fired close to the streamer sensors). *Inset* shows a photo of the streamer while moving to a new position in a forest track with uneven and loose sediments along part of profile 2. The wireless recorders (10–20 m apart) connected to 10 Hz geophones were spaced along the landstreamer array and fixed for the whole profile. Photos by Alireza Malehmir

The key acquisition parameters are summarized in Table S1 of the electronic supplementary material (ESM). Figure 7 shows two examples of shot gathers, after vertical stacking of the repeated shot records, from each profile. Most shot gathers have excellent data quality, except at a few places along profile 2 in the forest track (likely due to bad sensor coupling); water pumps along the forest tracks also generated noise at times during the acquisition.

Refraction and reflection data imaging

Data processing started with refraction seismic tomography given the quality of the first breaks particularly at far offsets. First breaks were picked automatically and manually corrected where needed. Refraction tomography was carried out using a diving-wave (or turning-ray) first break tomographic inversion method (Tryggvason et al. 2002) using cells of 2 and 1 m in horizontal and vertical directions; in the lateral direction cells were kept large to force the model to look 2D although the modeling uses a 3D algorithm for travel time calculations. For details about the tomographic velocity models, readers are referred to Table S1 and Fig. S1 of the ESM. The wireless sensors spaced along the entire length of each profile allowed the energy from the refracted waves to be recorded as far as 1 km notably improving both the investigation depth for the refraction tomography and the fold coverage at depth for the reflection data.

For the reflection data processing, a simple and conventional algorithm was chosen to avoid generating processing artefacts (Black et al. 1994; Steeples and Miller 1998). The algorithm is based on signal enhancement in the pre-stack data and CMP (common midpoint; 2-m spacing) stacking after normal moveout corrections. The most crucial processing step was the velocity analysis given the deep underground water table (about 20–50 m below ground level in some places), subsurface heterogeneity (subaqueous channels, kettle holes) and dipping bedrock in the study area. Indications of water-table reflections were noticeable in some shot gathers like the ones shown in Fig. 7 (the top red arrow). The seismic reflection processing flow is detailed in Table S2 in the ESM. In conjunction with the seismic survey a test was also conducted where planted MEMs sensors were placed next to the streamer sensors in order to check whether the landstreamer sensors had reliable and consistent travel time phases with the planted ones (Brodic et al. 2015). Checking the phase and amplitude of data was crucial for both reflection and refraction imaging but also for future studies using the landstreamer.

The heterogeneity within the sediments and bedrock undulations made the reflection imaging quite challenging particularly with the velocity analysis. It appeared that one set of reflections was very shallow (i.e. above water table) and another one was focused on the bedrock surface and the structures in its immediate vicinity. An approach tested before (Miller and Xia 1998; Juhlin et al. 2010; Malehmir et al. 2013a; Place et al. 2015) was to combine two different sets of reflections, by generating a stack focusing on very shallow reflections and another one focusing on bedrock reflections or below the water table. This gave the best results for profile 1 where 10–20 m deep shallow structures could be identified.

Data interpretation procedure

The interpretation of seismic reflections and their scale is guided by the hydrogeological units and more specifically the reference depositional model for the coarse-grained unit, which is based on previous studies (Fig. 3). This reference model forms also the base for the understanding of the groundwater environment and related flow model. The reference model shows three basic large-scale esker elements: esker core (glaciofluvial coarse-grained unit), MUKH structures (separate unit) and large-scale cross-bedded fan lobe channels (Baker 1973; Theakstone 1976) deposited towards the esker margins (glaciofluvial fine-grained unit). In addition to these, the remaining stratified esker sediments form the main bodies of the esker fans. These elements are the major

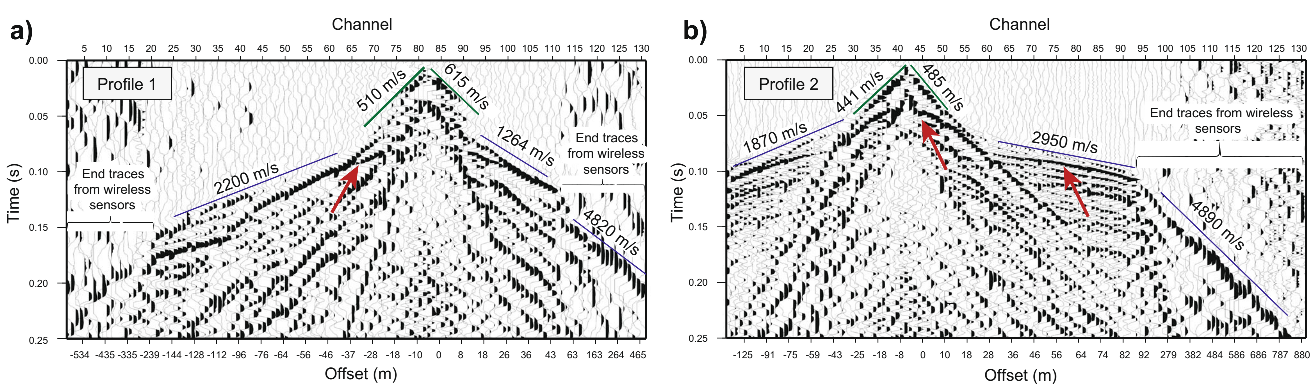

Fig. 7 Example raw shot gathers (after vertical stacking of the repeated shot records) and apparent velocities from **a** profile 1 and **b** profile 2. The *red arrows* indicate distinct reflections identifiable already in the raw data. The wireless sensors are noticeable at far offsets and tend to be in general noisier and have lower frequency content; however, the first breaks are identifiable almost on all traces. Note that for display purposes the offset distance between receivers is not scaled

hydrogeological features that affect the artificial recharge and groundwater flow within the MAR plant. The main reflection patterns identified from the 2 km of seismic reflection data can be interpreted as large-scale seismic facies (Fig. 8). The more detailed interpretation of the stratified esker fan sediments is inhibited by the resolution of the seismic data in relation to the small-scale complexity of the sediments. The interpretation of the elements or the seismic facies forms the basis for the zonation of the coarse-grained unit, which is relevant for the more detailed hydrogeological model.

Results and interpretations

Water table and bedrock surface

The results of seismic refraction tomography along the two lines are shown in Fig. 9. Available boreholes near (ca. 5–10 m) the profiles are projected into the tomography sections for comparison. The subsurface is characterized by rapid vertical velocity gradients where the water table is remarkably deep. Soft and dry unconsolidated sediments, like sand-dominated littoral deposits (1–10 m thick), are characterized by a low velocity (ca. 500 m/s) in the first few meters below the land surface. When the sediments become saturated (below water table or its vicinity) the seismic velocity makes a large increase to 1,500–1,800 m/s, which is typical for sandy or silty sediments (e.g., Malehmir et al. 2013a; Salas-Romero et al. 2016).

During the preparation of the seismic data, a clear reflection of about 500 m/s consistently appeared at shallow depths on most shot gathers after direct arrivals (see for example the top red arrow in Fig. 7a,b). This was judged to be from the transition zone where the unconsolidated sediments change from a dry state to a partially or completely water-saturated state. It is in general a sharp surface, clearly depicted in the velocity models being gently dipping towards the low land areas (Fig. 9). The water table at the time of the seismic survey (S. Saraperä, Turku Region Water Ltd, personal communication, 2014) is shown as a blue-white dashed line on the tomography sections and in most places matches well the tomography results; however, near surface velocities are expected to be extremely sensitive to the dry/saturated sediments interface found in the vicinity of the water table, therefore the velocity model does not follow the water-table boundary in some areas. This seems to be the case at the NW part of profile 1, especially at distance 200–300 m where the coarse-grained and conductive esker fan apex (borehole VI485) is expected to rise above the water table (Fig. 9a). The fan apex consists of 40 m-thick gravel with a 20-m intervening bed of sandy gravel (73–93 m a.s.l.) that holds the water table. Low velocity areas observed below the water table may be explained by dislocated sediments and MUKH structures, as for example in profile 1 (Fig. 9a) at 400–500 m distance or at 300–400 m distance along profile 2 (Fig. 9b), as deformed sediments do not have similar seismic velocity compared with undisturbed materials. Coarsest sediments are concentrated on the NE end of the profile 2 where the corresponding low-velocity zone due to unsaturated sediments is thicker from the contribution of surface topography (higher elevation). The water table was observed at 20–40 m depth in this part of the profile.

The bedrock surface is identified in the distinctly high (>5,000 m/s) velocity regions. For profile 1 (Fig. 9a), three boreholes intersect the bedrock (VI485, VI596, V566). Borehole VI596 hits fractured bedrock, and VI7 ends in gravel-dominated boulder-rich sediments (Fig. 9a). V566 hits the bedrock at 62.8 m a.s.l., while V550 ends in a silty bed at about 62 m a.s.l. The two distinct zones of high seismic velocities (> 5,000 m/s) match well with the bedrock as indicated by boreholes VI485 and VI566 near both ends of profile 1 (Fig. 9a). Bedrock surface can be reliably picked from the tomographic velocity model. The central part of profile 1 (300–600 m distance), where still relatively high velocities (> 3,000 m/s) are observed, represents a major fractured bedrock zone, manifested itself as a zone of bedrock depression. Velocities around 3,000 m/s indicate fractured/weathered bedrock (Barton 2007). This depression was also suggested by gravity surveys in the study area (Valjus 2006). For profile 2, boreholes VI282, VI285 and VI252 are drilled down to bedrock, while VI250 and VI6 end in bouldery sand and gravel, respectively (Fig. 9b). VI251 indicates a layer of till at 73 m a.s.l. A major depression in the bedrock is observed in the central part of the profile, around 300–400 m distance (Fig. 9b).

Description and interpretation of seismic profile 1

Profile 1 is divided into 4 zones based on the reflection patterns or large-scale seismic facies (Fig. 10b, c). The bedrock level in the NW end of the profile (zone 1) is roughly at 50–60 m a.s.l. The sediments here show chaotic and dislocated (deformed) reflections in association with concave large-scale geometry and comprise a large-scale seismic facies unit (small MUKH structures) that is partly in contact with the arched stratified facies and the bedrock. Seismic facies (Fig. 8) with arched geometry in contact with the bedrock (ca. 50 m thick at the 200–300 m distance) indicates the architecture of the esker core as supported by the borehole data (VI485).

Zone 2 exhibits a steep drop in the bedrock level associated with vertically dislocated strong reflections at 300–350 m distance from the line beginning that are related to the highly fractured margin of the wider fractured bedrock zone. The reflections within zone 2 indicate coarse-grained materials but are difficult to interpret; however, the zone can be divided roughly in two parts. The lower part below 70 m a.s.l. contains sediments filling the fractured zone, whereas the upper part on the SE side of the esker core contains mainly horizontal

Seismic facies	Characteristics	Lithology	Sedimentological interpretation and hydrogeological implication
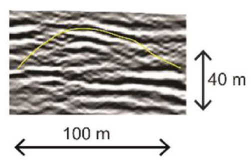	Arched geometry, convex reflections; stratified high amplitude or non-stratified low amplitude reflections and discontinuous nature, lower boundary with bedrock contact.	Bouldery gravel	Esker core of typical dimensions formed by meltwater flow in subglacial tunnel ➔ High hydraulic conductivity, main aquifer, groundwater pumping stations.
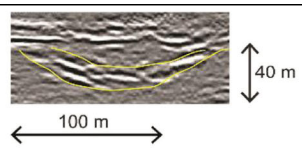	Concave large-scale geometry, various amplitude reflections, discontinuous/dislocated reflections, marginal unconformities and bedrock contact.	Mixed sediments with fine-grained beds	MUKH –structure with large-scale deformation, lateral to esker core ➔ Restricts and guides groundwater flow with longer residence times, possibilities for reverse gradients from infiltration.
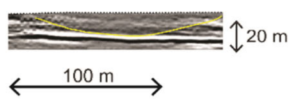	Large trough-shaped geometry, weakly stratified, low amplitude to transparent reflections, truncates sediments below.	Relatively homogeneous sand to gravel sediments	Major channels of subaqueous fan lobes, often with large-scale cross bedded fill. ➔ If associated with infiltration ponds, they direct the water flow affecting residence times.
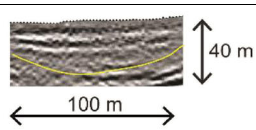	Large concave geometry, thick and stratified, low to moderate amplitude reflections, in contact with the arched esker core facies, truncates sediments below.	Gravel and sand sediments	Proximal channelized subaqueous fan sediments adjacent to the esker core ➔ High hydraulic conductivity
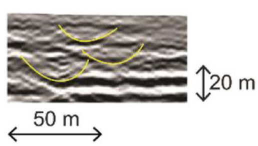	Mainly horizontal or low angle moderate to low amplitude reflections, mainly continuous reflections, sometimes with trough-shaped sets truncating sediments below.	Silt to sand and gravel sediments	Subaqueous fan (body) sediments with small channels (cut and fill) or mass flow deposits, fine-grained lower fan sediments. ➔ Intermediate conductivity, infiltration pond locations and important for residence times.
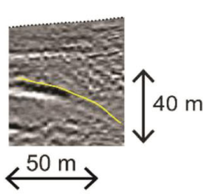	Stratified, low to moderate amplitude reflections, toplap to uppermost horizontal sediments. Lower part non-stratified with poor reflections. Erosional unconformity to fan body sediments. Poor facies coverage by the survey.	Sand to gravel and diamicton below	Crevasse deposits (subaqueous) of the main interlobate ridge in glacial bay superimposed on the esker fan sediments. Possible large-scale cross bedded sets underlain by mass-flow diamicton ➔ They affect groundwater flow patterns as revealed by water chemistry.
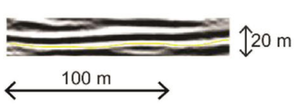	Strong, high amplitude reflections, horizontal and continuous, 10-20 m thick unit, lower boundary with bedrock contact	Diamicton	Subglacial till (also below the esker core) ➔ Poor hydraulic conductivity, fills the major fracture zone below the high-conductivity esker deposits
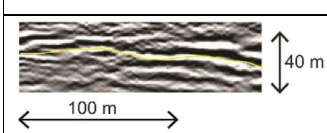	Strong, high amplitude reflections, mainly continuous, undulated	Bedrock contact	Bedrock surface ➔ Boundary for groundwater flow models
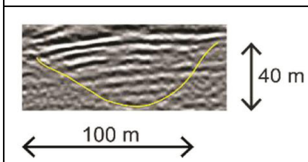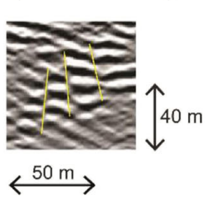	(top) Concave geometry in bedrock and especially below esker core facies, horizontal/continuous high to intermediate amplitude reflections. (bottom) Dislocated/faulted high amplitude reflections in bedrock.	(top) Basement rocks (bottom) Possible remnant of Jothnian sandstone within the fracture valley	(top) Fractured bedrock with only horizontal fracturing reflected ➔ It assists to high hydraulic conductivity below the esker core/main aquifer. (bottom) Faulted fracture valley margin ➔ Adjacent to poorly conductive till beds, hydrogeological continuity and importance not known.

Fig. 8 Seismic facies and their interpretation

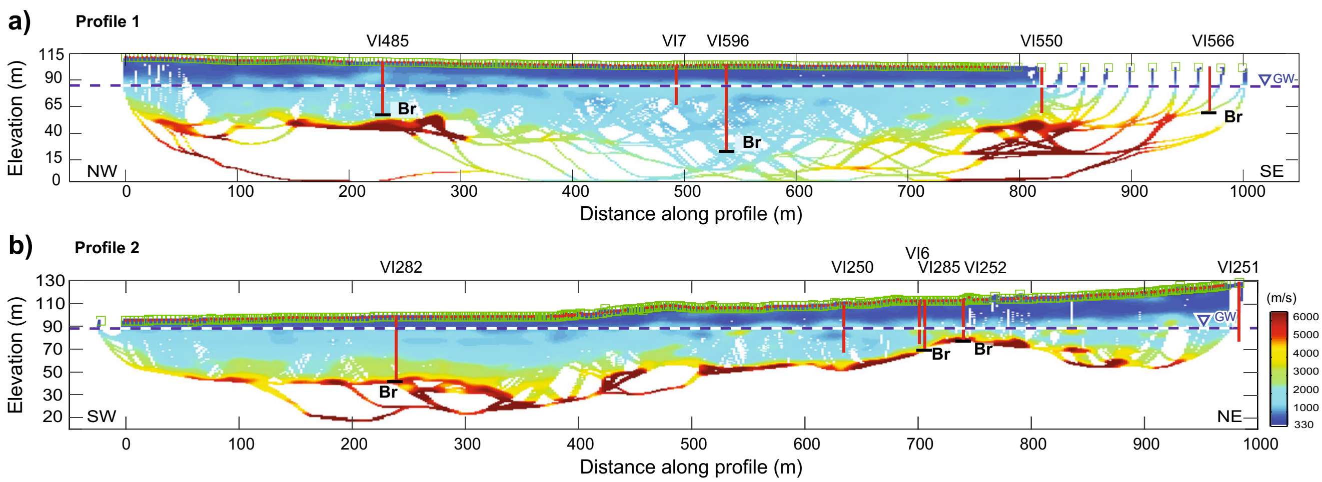

Fig. 9 Seismic refraction tomography sections along a profile 1 and b profile 2. Boreholes near the profiles are indicated using red bars. Awide bedrock fracture zone is estimated from 300 to 600 m distance along profile 1. The depth to bedrock indicated by the boreholes matches well the increased seismic velocity (> 5,000 m/s). The blue dashed line represents the water table at the time of the seismic acquisition (July 2014), matching well the velocity transition from 400–500 to 1,500–1,800 m/s

reflections from stratified sediments with trough-shaped structures. The seismic facies in the upper part is interpreted as subaqueous esker fan sediments (Fig. 8).

Zone 3 includes the ca. 200-m-wide bedrock fracture zone, the bottom of which is at 10–15 m a.s.l. The seismic facies with strong horizontal reflections varying in thickness (up to 30 m) above the bedrock extends across the fractured zone (Fig. 8) and is interpreted as diamicton, probably till, as supported by stratigraphy and boreholes VI568 and VI596 within the fractured zone. This facies is overlain by the esker core (slightly arched geometry

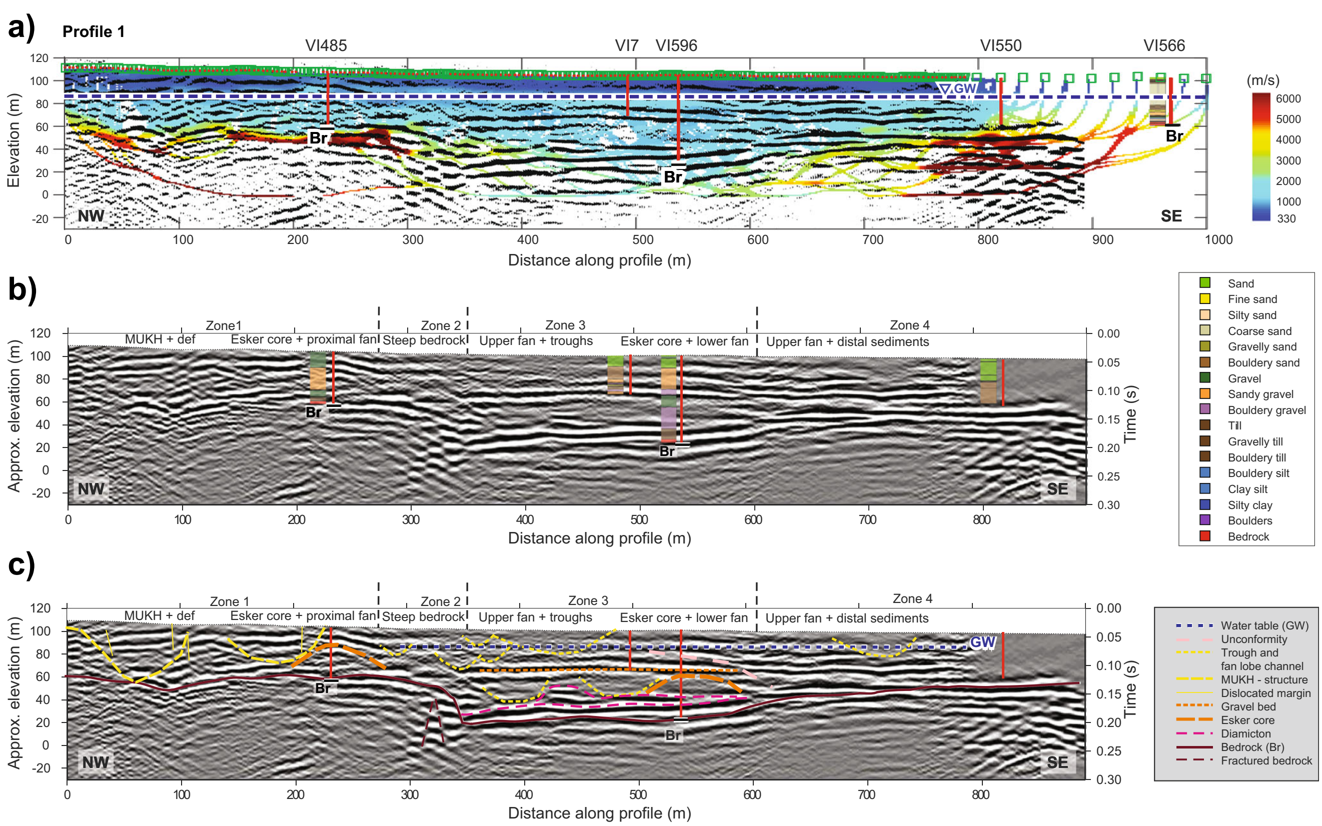

Fig. 10 **a** Seismic reflection (unmigrated but time to depth converted using a constant velocity of 1,000 m/s) section along profile 1 with the projected tomography section on top, including existing borehole data (indicated with *red bars*); **b** the seismic reflection section with interpreted depositional zones, borehole stratigraphy and indication of bedrock from the boreholes; **c** the interpretation of depositional units and indication of bedrock from boreholes along profile 1

facies) consisting of bouldery gravel (VI596) and two esker fan lobe channels (large trough-shaped weakly stratified facies on its NW side). The weak boundary separating the facies indicates similar coarse-grained materials; however, the discontinuous reflection between the troughs and partly below the esker core might indicate the existence of two different diamictons. The esker fan lobe channels were formed within the bedrock fracture valley and later covered by subsequent esker fan sediments. The esker core is about 20 m thick, but the shape of the core is not distinctly arched due to the diagonal position relative to profile 1.

The shallowest part of zone 3 includes a continuous horizontal reflection at ca. 60–70 m a.s.l. above the esker core and the large trough-shaped facies, and is partly truncated by the narrow troughs of zone 2 (subaqueous fan body sediments, Fig. 8) and overlain by other horizontal reflections in zone 4. It extends across the fractured bedrock until the unconformity at the SE-end of the zone, it indicates a change from sandy to bouldery gravel as observed in borehole VI596 (at 68–73 m a.s.l.) and is characterized as esker fan sediments (Fig. 10c). An indication of the water table at 86 m a.s.l. is seen within the fan sediments.

Zone 4 is located outside the fractured bedrock and comprises mainly horizontal reflections that are truncated in the upper part by the about 100-m-wide trough-shaped facies similar to those in zone 3. Boreholes indicate sand-dominated sediments with intercalation of fine-grained sediments close to the bedrock surface (VI550). The seismic facies of zone 4 are interpreted as esker fan sediments. The trough-shaped facies represent fan lobe channels.

Description and interpretation of reflection seismic profile 2

Profile 2 is perpendicular to the esker system and lies across the coarse-grained hydrogeological unit (main aquifer) at its widest point in zone 3 (Fig. 1). Based on the bedrock level interpretation, the thickness of the deposits varies between 40 and 70 m (Fig. 11c). The shallow strong reflection just below 90 m a.s.l. at the SW-end of the profile is indicative of the water table (ca. 88 m a.s.l.) The profile is divided into 5 zones based on the different reflection characteristics (Fig. 11b, c). The uppermost part of the profile 2 first shows an erosional unconformity that is overlain by the topmost shore deposits as observed from the nearby pit exposures. Starting with zone 2 towards the northeast, the uppermost part is characterized by a continuous, moderate-amplitude reflection that is slightly distorted by a concave unconformity between 800 and 850 m, extending to the bedrock. This continuous moderate-amplitude reflection and the overlying homogeneous unit lacking reflectivity are associated with the last depositional stages of the interlobate complex covered by the shore deposits.

Zone 1 runs along the tributary esker core (Fig. 1) towards the northeast following the margin of the bedrock deepening

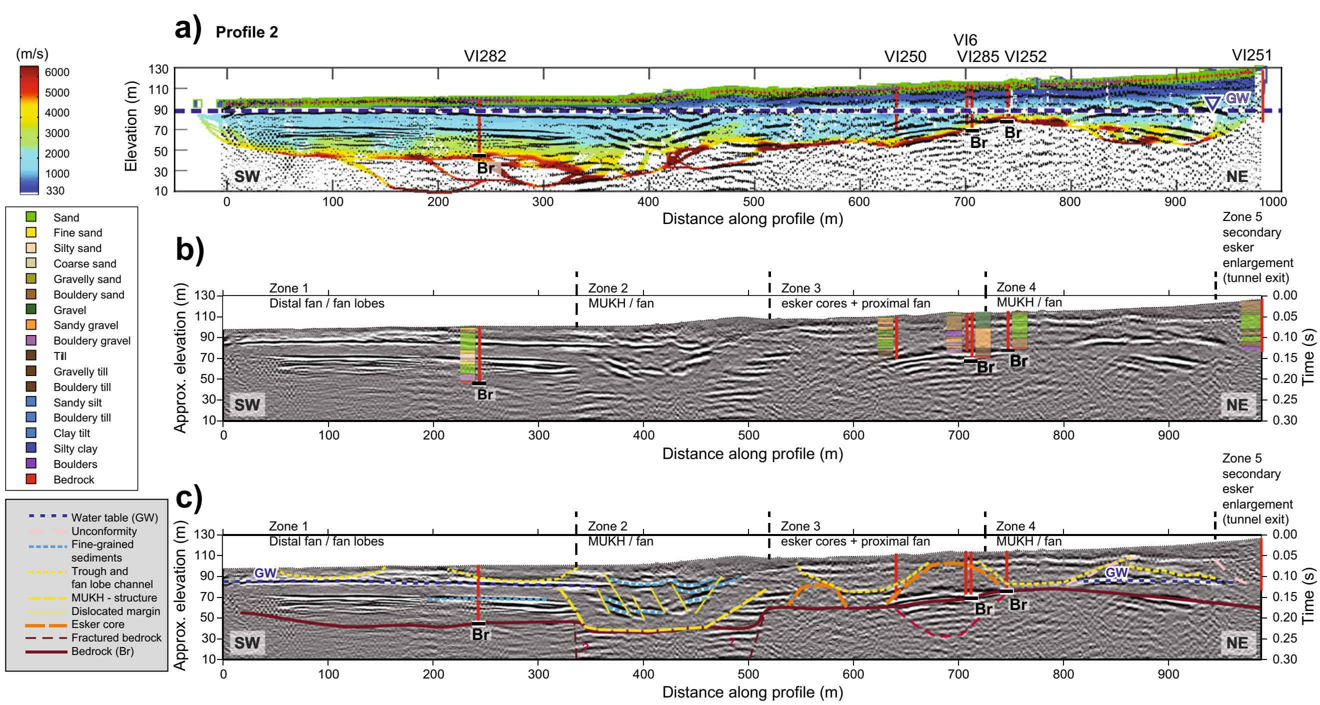

Fig. 11 **a** Seismic reflection (unmigrated but time to depth converted using a constant velocity of 800 m/s) section along profile 2 with the projected tomography section on top, including existing borehole data near the profile; **b** the seismic reflection section with interpreted depositional zones, borehole stratigraphy and indication of bedrock from the boreholes; **c** the interpretation of depositional units and indication of bedrock from boreholes along profile 2

at 45–50 m level (Mäkinen (2003b). Gravel-dominated materials in borehole VI275 (ca. 50 m northwest of the profile) support the presence of the tributary esker. The reflections below the water table are mainly horizontal with stronger reflections at ca. 60–70 m a.s.l., which correspond to silty sand (borehole VI282). The silty-sand unit is underlain by a vaguely convex package, up to 20 m thick, at 250–350 m distance along the profile. According to borehole VI282, this reflection corresponds to sand and stony (bouldery) gravel that is known to scatter the seismic signal, and thus the underlying bedrock is not observed as a clear continuous reflection. The uppermost sediments above the water table consist of horizontal reflections truncated by 10–15-m-thick and over 100-m-wide trough-shaped facies (Fig. 8). Zone 1 is interpreted to represent esker fan sediments. Beds of bouldery gravel at 43–50 m a.s.l. and sand at 50–59 m level a.s.l. (VI282) correspond to lower proximal tributary fan sediments, whereas the uppermost trough-shaped reflections show cross-bedded fan lobe channels from the main esker as indicated by the previous observations from the nearby aggregate pits (Figs. 5a and 8). However, the detailed understanding of the contact between the tributary esker fans and the main esker fans remains poor.

Zone 2 is characterized by a major ca. 200-m-wide and up to 70 m-thick concave feature extending down to bedrock (Fig. 8). Comparison with the tomography results supports the presence of a major low-velocity depression in this part of the profile (Fig. 11a). The bottom part appears as a zone lacking reflectivity while the middle part shows complex and discontinuous/dislocated reflectivity. The reflections associated with the bedrock geometry form a seismic facies interpreted as a large MUKH structure with collapsed/deformed esker fan sediments (illustrated also in Fig. 5b). These large MUKH structures typically occur on both sides of the esker core and in many places along the esker at the margins of the coarse-grained hydrogeological unit. The reflection seismic section along profile 2 provides the first reliable evidence for the hypothesized bedrock contact of the large MUKH-structures, which is encouraging.

On the northeast side of the large MUKH-structure, zone 3 shows two arched structures with vague inner reflections separated by a large concave geometry seismic facies with reflections indicating thick stratified beds (Fig. 8). The arched geometry facies at 700 m distance is mainly composed of stony and sandy gravel as indicated by boreholes VI6 and VI285. This gravel facies is underlain by a concave geometry with horizontal reflections in the bedrock (Fig. 8). The arched facies are interpreted as bouldery esker core sediments, where the core at 700 m represents the known position of the main esker core, while the core at 550 m is associated with the previously undetected tributary esker core., suggesting that the two esker cores join a bit further towards the southeast. Based on the depositional model, the trough-shaped structure between the cores might be interpreted as a proximal fan structure. Zone 3 forms the main aquifer of the glaciofluvial complex. The thick concave geometry facies between the esker cores is interpreted as a proximal fan structure. Horizontal reflections below the main esker core indicate intense fracturing due to pressurized meltwater flow in the subglacial tunnel. This is an important interpretation, because it suggests that the aquifer extends down to bedrock, typical for an esker environment.

Zone 4 is characterized by a large concave geometry seismic facies with vaguely dislocated reflections below the uppermost continuous intermediate reflection. The eastern side of the facies shows an unconformity that extends down to bedrock. The reflections below the unconformity show low-angle reflections dipping to the NE. The sediments bordered by the esker core and the concave unconformity are interpreted to represent the SE-end of a second large MUKH structure as supported by the previous studies (Mäkinen 2003b). The low-angle sediments on the NE side of the MUKH structure exhibit undeformed esker fan sediments. The strong reflector roughly at 90 m a.s.l. indicates the water table. Bedrock surface is picked up again as a strong reflection similar to that observed below the esker core within zone 3.

Profile 2 ends close to the highest part of the Säkylänharju ridge, where zone 5 reveals a marked change in seismic facies with a set of toplap reflections (Fig. 8) in sandy deposits underlain by diamicton (VI251). The toplap reflections stop at the uppermost continuous intermediate reflection and resemble large-scale cross-bedding that dip parallel to the main ridge. These deposits are related to the meltwater flows along the interlobate crevasse forming the widening of the coarse-grained hydrological unit (Artimo et al. 2003). The diamicton below the crevasse deposits might represent mass-flow deposits lateral to the esker fan sediments.

Discussion

Due to the complex and heterogeneous subsurface, the depositional structures at Virttaankangas are characterized by large vertical velocity gradients over short depths, which is further complicated when the unconsolidated sediments make the transition to the water-saturated zone. As the water-table zone is approached, velocities are especially sensitive and can vary from just a few hundreds of meter per second to an increase of four times or more (Bachrach and Nur 1998). Additionally, the complex depositional environment such as esker cores, MUKH structures and fan lobe channels as well as the fractured bedrock lead to lateral velocity variations. Even though in shallow seismic surveys reflections from the water table are not always common (Steeples and Miller 1998), one can notice these reflections here distinctly in the shot gathers (e.g. Fig. 7) and with some interruption in the stacked sections as well. Given the shallow depth of investigation and the characteristic challenges associated with near-surface structures in seismic reflection data (Frei et al. 2015), the processing focused on imaging the rapidly lateral/vertical variations in the shallow structures above the bedrock. After an extensive velocity analysis during data processing, constant velocities were used for the final time to depth conversion of the seismic sections (1,000 m/s for profile 1 and 800 m/s for profile 2). Some errors are expected (on the order of a few meters) in the depth position of the reflections given the rapid velocity change with depth in the study area; however, the refraction section together with a good knowledge of the depositional environment from existing data help limit this uncertainty. The bedrock surface is interpreted from the high amplitude continuous deep reflections even though at places the bedrock reflection is lost underneath gravel and sand beds, as the seismic signal can easily be scattered in such an environment.

The seismic results of the Virttaankangas area confirm the location and dimensions of the esker core that is the main aquifer and the target for the pumping stations of the MAR plant. The esker core facies has a distinct arched shape due to esker deposition in an R-channel (Röthlisberger 1972) resting on hard crystalline bedrock. The character of the reflections, high amplitudes and discontinuous nature, can characterize coarse-grained sediments that are likely indicative of esker cores (Pugin et al. 2009a). The results confirm that continuous and thick till beds below the esker core within the fractured bedrock zone form poorly conductive sediments that are important for the groundwater flow model, but it was revealed that the till beds were partly eroded during the esker deposition lateral to the main core. This indicates a proximal fan deposition and wide high conductivity zone within a constrained environment of the fractured bedrock (Fig. 12a). The position of the tributary esker along profile 2 is a new finding in this study (Fig. 12b) and will improve the high hydraulic conductivity close to the main core. Its position is also supported by very short residence times for infiltrated water in that area (Aki Artimo, Turku Region Water Ltd, personal communication, 2016). The new seismic data also suggest high conductivity in fractured bedrock structure below the esker core.

Earlier studies indicated the presence of large MUKH structures on the sides of the esker core with suggested bedrock contact (Mäkinen 2003b). This study now confirms the large dimensions of the MUKH structures and their contact to bedrock (Fig. 12). The results also show their complex deformed internal structure restricting the groundwater flow with increased residence times of the infiltrated water. These MUKH structures are described in

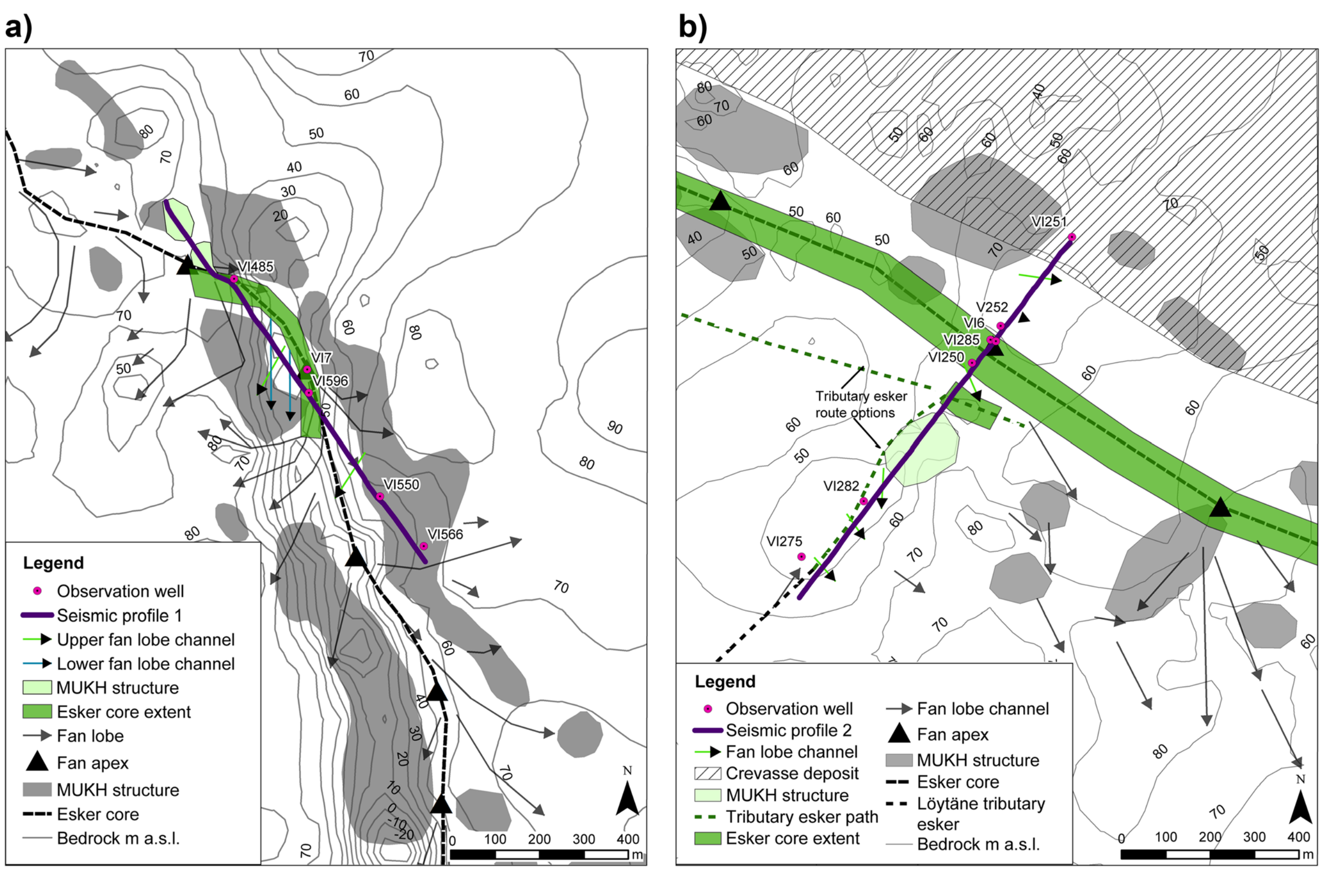

Fig. 12 The interpreted main esker elements (esker core, fans, MUKH structures; *shown in color*) and bedrock characteristics based on profile 1 compared to the earlier research (Mäkinen 2003b; shown in *grayscale*) for **a** profile 1 and **b** profile 2. Bedrock elevation contours modified from Valjus (2006)

the groundwater flow model with specific parameters and have been used for the artificial infiltration and the creation of inverse gradients. The fan lobe channels, their lateral extents and relationship to the highly conductive esker core were shown with adequate detail in this study. Two previously unknown fan lobes lateral to the main esker core were identified within the bedrock fracture zone. The contact between the secondary esker enlargement deposits and the esker fans was better identified near the top of the main ridge, which strengthens the delineation of the wider coarse-grained hydrogeological unit (Fig 12b).

The novel high-resolution landstreamer seismic survey offered valuable and continuous depth information down to bedrock and was capable of detecting main structures associated with the stratigraphically and hydrogeological relevant units in complex interlobate esker deposits. Thus, the method is highly cost-effective over wide study areas with enough paths/roads, where inadequate sedimentological and lithological data hinder reliable correlation; furthermore, if the thickness of the deposits exceeds about 40 m or if the surficial sediments are not suitable for GPR survey (e.g., clay rich and saturated), the high-resolution seismic method can stand alone. However, if a more detailed sedimentological understanding or local depositional model is needed (e.g. for detailed groundwater flow modeling) the method should still be combined with GPR surveys if possible. Given that there is enough space for maneuvering the source, and coupling conditions are fulfilled, a survey could be carried out in a sparse layout in forests as well, particularly by using wireless recorders. Peat bogs or peatlands, and generally thick layers of soft vegetation, would greatly attenuate the seismic signal and are known to be challenging environments for seismic surveys (Miller et al. 1992). They are, however, part of the esker environments, and studies on MAR require surveys that image the whole aquifers area (Rossi et al. 2014). GPR measurements are known to successfully image peatlands (Comas et al. 2004; Lowry et al. 2009) but keeping in mind GPR's limited penetration depth, a high-resolution seismic survey will allow a reliable delineation of the esker systems with the surrounding wetlands.

As esker cores, esker fans included, can reach up to 500 m width, and accounting for the surroundings plains, landstreamer surveys are suitable for efficiently covering long distances. Streams or springs that require an interruption in the seismic line are accounted for with wireless recorders that assure continuity in the survey line. Defining the hydrogeological units of the aquifers from boreholes only and open pits is risky due to uncertainty in these sparse data that assume continuous units. An entire aquifer can be sampled in one seismic campaign (in 1 week for example) and a combined geophysical-hydrogeological modelling strategy will yield an improved image compared to any of the approaches taken separately (Rubin et al. 1992). Seismic sections display continuous profiles of one (or several) km where complementary data can be overlaid and provide control for the interpretation.

Conclusions

Two ca. 1-km-long seismic profiles were successfully acquired over a relatively thick complex and heterogeneous glacial environment, at Virttaankangas, Finland. The 200-m-long prototype landstreamer system was tested for its suitability for hydrogeological characterization of the complex interlobate esker deposits down to bedrock. High quality refraction and reflection seismic data were acquired in an efficient survey combining the landstreamer and wireless recorders that proved crucial in providing information from more than 100 m-thick bedrock glacial cover. Data processing had to account for a challenging setting in terms of a deep water table at certain locations (ca. 40 m) and rapid changes in the depositional environment. The aquifer features were identified from a combination of reflection imaging and refraction tomography results allowing a good control and complementary interpretation of the results.

Besides the bedrock surface, the refraction seismic results confirm a zone of fractured bedrock where the velocities are around 3,000 m/s. The correlation between the tomography and the reflection seismic sections provides a good overview of the sedimentary structures along each profile. Further, the sections are rich in reflectivity and hence they allow comparison to the existing depositional model with a delineation of the main architectural elements relevant for the hydrogeological model as well as for groundwater flow modelling down to the bedrock level.

The main findings of this study are valuable for the future sustainable use of the aquifer and are summarized as following:

- The cost- and time-effective seismic survey enabled the characterization of the hydrogeologically relevant large-scale esker architectural elements that impact the groundwater infiltration and flow.
- Seismic facies were used to improve the determination of hydraulic conductivity distribution in the groundwater flow model down to bedrock level. This also promoted the integration of scattered geological data for modelling purposes.
- Deep fractured bedrock with complex overlying stratigraphy was delineated and the hydraulic connection between the hydraulically conductive unit and bedrock was shown.
- New data enable accurate planning for future pumping wells and infiltration areas in the most complex and widest part of the coarse-grained unit (within the esker core sediments).

- The combination of seismic and GPR surveys together with neighboring borehole information within thick and widespread glaciofluvial deposits provides the best approach for accurate depositional models with minimized need for borehole reference.

Acknowledgements The authors would like to thank Trust 2.2 (http://www.trust-geoinfra.se) Formas project (252-2012-1907) under which this test survey was initiated. Turku Region Water Ltd, the Geological Survey of Finland (GTK) and University of Turku/Dept. of Geography and Geology sponsored the data acquisition and collaborated in this project. Graduate students from Uppsala University participated in the fieldwork for which the authors are grateful. A. Tryggvason (Uppsala University) is thanked for providing the PStomo_eq available to use for travel time tomography. GLOBE Claritas™ under license from the Institute of Geological and Nuclear Sciences Limited, Lower Hutt, New Zealand, was used to process the seismic data. We are thankful for valuable and critical comments provided by Dr. David Sharpe and two anonymous reviewers that together with the editor helped improve the quality of the paper.

References

Almholt A, Wisén R, Jorgensen R, Ringgaard J, Nielsen U (2013) High resolution 2D reflection seismic land streamer survey for groundwater mapping: case study from southeast Denmark. In: SEG Technical Program Expanded Abstracts 2013. Society of Exploration Geophysicists, Tulsa, OK, pp 1894–1898

Artimo A, Mäkinen J, Berg RC, Abert CC, Salonen VP (2003) Three-dimensional geologic modeling and visualization of the Virttaankangas aquifer, southwestern Finland. Hydrogeol J 11: 378–386. doi:10.1007/s10040-003-0256-6

Artimo A, Saraperä S, Ylander I (2008) Methods for integrating an extensive geodatabase with 3D modeling and data management tools for the Virttaankangas Artificial Recharge Project, southwestern Finland. Water Resour Manag 22:1723–1739. doi:10.1007/s11269-008-9250-z

Artimo A, Saraperä S, Puurunen O, Mäkinen J (2010) The Turku Region Artificial Infiltration Project, Finland: tools for enhanced aquifer characterization. ISMAR, Abu Dhabi, United Arab Emirates, pp 93–100

Bachrach R, Nur A (1998) High-resolution shallow-seismic experiments in sand, part I: water table, fluid flow, and saturation. Geophysics 63: 1225–1233. doi:10.1190/1.1444423

Baker G, Steeples D, Schmeissner C, Spikes K (2000) Collecting seismic-reflection data from depths shallower than three meters. In: Symposium on the application of geophysics to engineering and environmental problems 2000. Environment and Engineering Geophysical Society, Denver, CO, pp 1207–1214

Baker VR (1973) Paleohydrology and sedimentology of Lake Missoula flooding in Eastern Washington. In: Geological society of America special papers. Geological Society of America, Boulder, CO, pp 1–73

Banerjee I, McDonald B (1975) Nature of esker sedimentation. In: Jopling AV, McDonald BC (eds) Glaciofluvial and glaciolacustrine sedimentation. Society of Economic Paleontologists and Mineralogists, Tulsa, OK

Barton N (2007) Rock quality, seismic velocity, attenuation and anisotropy. CRC, Auckland, New Zealand

Black RA, Steeples DW, Miller RD (1994) Migration of shallow seismic reflection data. Geophysics 59:402–410. doi:10.1190/1.1443602

Boucher C, Pinti DL, Roy M, Castro MC, Cloutier V, Blanchette D, Larocque M, Hall CM, Wen T, Sano Y (2015) Groundwater age investigation of eskers in the Amos region, Quebec, Canada. J Hydrol 524:1–14. doi:10.1016/j.jhydrol.2015.01.072

Bouwer H (2002) Artificial recharge of groundwater: hydrogeology and engineering. Hydrogeol J 10:121–142. doi:10.1007/s10040-001-0182-4

Bradford JH (2002) Depth characterization of shallow aquifers with seismic reflection, part I: the failure of NMO velocity analysis and quantitative error prediction. Geophysics 67:89–97. doi:10.1190/1.1451362

Brennand TA (2000) Deglacial meltwater drainage and glaciodynamics: inferences from Laurentide eskers, Canada. Geomorphology 32: 263–293. doi:10.1016/S0169-555X(99)00100-2

Brodic B, Malehmir A, Juhlin C, Dynesius L, Bastani M, Palm H (2015) Multicomponent broadband digital-based seismic landstreamer for near-surface applications. J Appl Geophys 123:227–241. doi:10.1016/j.jappgeo.2015.10.009

Burke MJ, Brennand TA, Perkins AJ (2012) Evolution of the subglacial hydrologic system beneath the rapidly decaying Cordilleran Ice Sheet caused by ice-dammed lake drainage: implications for meltwater-induced ice acceleration. Quat Sci Rev 50:125–140. doi:10.1016/j.quascirev.2012.07.005

Burke MJ, Woodward J, Russell AJ, Fleisher PJ, Bailey PK (2008) Controls on the sedimentary architecture of a single event englacial esker: Skeiðarárjökull, Iceland. Quat Sci Rev 27:1829–1847. doi:10.1016/j.quascirev.2008.06.012

Comas X, Slater L, Reeve AS (2004) Geophysical evidence for peat basin morphology and stratigraphic controls on vegetation observed in a Northern Peatland. J Hydrol 295:173–184. doi:10.1016/j.jhydrol.2004.03.008

Comas X, Slater L, Reeve AS (2011) Pool patterning in a northern peatland: geophysical evidence for the role of postglacial landforms. J Hydrol 399:173–184. doi:10.1016/j.jhydrol.2010.12.031

Dillon P (2005) Future management of aquifer recharge. Hydrogeol J 13: 313–316. doi:10.1007/s10040-004-0413-6

Finnish Environment Institute (2016) Ground water areas 1: 20 000. Spatial datasets. http://www.syke.fi/openinformation

Francese R, Giudici M, Schmitt DR, Zaja A (2005) Mapping the geometry of an aquifer system with a high-resolution reflection seismic profile. Geophys Prospect 53:817–828

Frei W, Bauer R, Corboz P, Martin D (2015) Pitfalls in processing near-surface reflection-seismic data: beware of static corrections and migration. Lead Edge 34:1382–1385. doi:10.1190/tle34111382.1

Giustiniani M, Accaino F, Picotti S, Tinivella U (2008) Characterization of the shallow aquifers by high-resolution seismic data. Geophys Prospect 56:655–666. doi:10.1111/j.1365-2478.2008.00705.x

Gorrell G, Shaw J (1991) Deposition in an esker, bead and fan complex, Lanark, Ontario, Canada. Sediment Geol 72:285–314. doi:10.1016/0037-0738(91)90016-7

Hebrand M, Åmark M (1989) Esker formation and glacier dynamics in eastern Skane and adjacent areas, southern Sweden. Boreas 18:67–81. doi:10.1111/j.1502-3885.1989.tb00372.x

Huddart D, Bennett MR, Glasser NF (1999) Morphology and sedimentology of a high-arctic esker system: Vegbreen, Svalbard. Boreas 28: 253–273. doi:10.1111/j.1502-3885.1999.tb00219.x

Huuse M, Lykke-Andersen H, Piotrowski JA (2003) Geophysical investigations of buried Quaternary valleys in the formerly glaciated NW European lowland: significance for groundwater exploration. J Appl Geophys 53:153–157. doi:10.1016/j.jappgeo.2003.08.003

Jokela P, Kallio E (2015) Sprinkling and well infiltration in managed aquifer recharge for drinking water quality improvement in Finland. J Hydrol Eng 20, B4014002. doi:10.1061/(ASCE)HE.1943-5584.0000975

Juhlin C, Dehghannejad M, Lund B, Malehmir A, Pratt G (2010) Reflection seismic imaging of the end-glacial Pärvie Fault system, northern Sweden. J Appl Geophys 70:307–316. doi:10.1016/j.jappgeo.2009.06.004

Juhlin C, Palm H, Müllern C-F, Wållberg B (2002) Imaging of groundwater resources in glacial deposits using high-resolution reflection seismics, Sweden. J Appl Geophys 51:107–120

Korsman K, Koistinen T, Kohonen G, Wennerström M, Ekdahl H, Honkamo M, Idman H, Pekkala Y (eds) (1997) Bedrock map of Finland 1: 1 000 000. Geological Survey of Finland, Espoo, Finland

Kruppenbach JA, Bedenbender JW (1975) United States patent: 3923121—towed land cable. US Patent and Trademark Office, Alexandria, VA

Kujansuu R, Kurkinen I, Niemelä J (1995) Glaciofluvial deposits in Finland. In: Ehlers J, Kozarski S, Gibbard PL (eds) Glacial deposits in North-East Europe. Balkema, Rotterdam, The Netherlands, pp 77–84

Lowry CS, Fratta D, Anderson MP (2009) Ground penetrating radar and spring formation in a groundwater dominated peat wetland. J Hydrol 373:68–79. doi:10.1016/j.jhydrol.2009.04.023

Mäkinen J (2003a) Time-transgressive deposits of repeated depositional sequences within interlobate glaciofluvial (esker) sediments in Köyliö, SW Finland. Sedimentology 50:327–360. doi:10.1046/j.1365-3091.2003.00557.x

Mäkinen J (2003b) The development of depositional environments within the interlobate Säkylänharju-Virttaankangas Glaciofluvial Complex in SW Finland. Suomalainen Tiedeakatemia, Helsinki, Finland

Mäkinen J, Räsänen M (2003) Early Holocene regressive spit-platform and nearshore sedimentation on a glaciofluvial complex during the Yoldia Sea and the Ancylus Lake phases of the Baltic Basin, SW Finland. Sediment Geol 158:25–56. doi:10.1016/S0037-0738(02)00240-3

Malehmir A, Bastani M, Krawczyk C, Gurk M, Ismail N, Polom U, Persson L (2013a) Geophysical assessment and geotechnical investigation of quick-clay landslides: a Swedish case study. Surf Geophys. doi:10.3997/1873-0604.2013010

Malehmir A, Saleem MU, Bastani M (2013b) High-resolution reflection seismic investigations of quick-clay and associated formations at a landslide scar in southwest Sweden. J Appl Geophys 92:84–102. doi:10.1016/j.jappgeo.2013.02.013

Malehmir A, Wang S, Lamminen J, Bastani M, Vaittinen K, Juhlin C, Place J (2015a) Delineating structures controlling sandstone-hosted base-metal deposits using high-resolution multicomponent seismic and radio-magnetotelluric methods: a case study from northern Sweden. Geophys Prospect 63:774–797. doi:10.1111/1365-2478.12238

Malehmir A, Zhang F, Dehghannejad M, Lundberg E, Döse C, Friberg O, Brodic B, Place J, Svensson M, Svensson M (2015b) Planning of urban underground infrastructure using a broadband seismic landstreamer: tomography results and uncertainty quantifications from a case study in southwestern Sweden. Geophysics 80:B177–B192. doi:10.1190/geo2015-0052.1

Malehmir A, Socco LV, Bastani M, Krawczyk CM, Pfaffhuber AA, Miller RD, Maurer H, Frauenfelder R, Suto K, Bazin S, Merz K, Dahlin T (2016a) Near-surface geophysical characterization of areas prone to natural hazards: a review of the current and perspective on the future. Adv Geophys 57:229–312. doi:10.1016/bs.agph

Malehmir A, Andersson M, Mehta S, Brodic B, Munier R, Place J, Maries G, Smith C, Kamm J, Bastani M, Mikko H, Lund B (2016b) Post-glacial reactivation of the Bollnäs fault, central Sweden: a multidisciplinary geophysical investigation. Solid Earth 7:509–527. doi:10.5194/se-7-509-2016

Miller P, Shaw GH, Glaser P, Siegel D (1992) Bedrock topography beneath the Red Lake peatlands. Geol Soc Am Abstracts with Programs 24:7

Miller R, Steeples D, Brannan M (1989) Mapping a bedrock surface under dry alluvium with shallow seismic reflections. Geophysics 54:1528–1534. doi:10.1190/1.1442620

Miller RD, Xia J (1998) Large near-surface velocity gradients on shallow seismic reflection data. Geophysics 63:1348–1356. doi:10.1190/1.1444436

Nadeau S, Rosa E, Cloutier V, Daigneault R-A, Veillette J (2015) A GIS-based approach for supporting groundwater protection in eskers: application to sand and gravel extraction activities in Abitibi-Témiscamingue, Quebec, Canada. J Hydrol Reg Stud 4(Part B): 535–549. doi:10.1016/j.ejrh.2015.05.015

National Land Survey of Finland (2010) Base map 1: 20 000. Sheet M3331L. NLS File service of open data. https://tiedostopalvelu.maanmittauslaitos.fi/tp/kartta?lang=en. Accessed December 2016

National Land Survey of Finland (2016) General map 1: 1000 000. NLS File service of open data. http://tiedostopalvelu.maanmittauslaitos.fi/tp/kartta?lang=en

Pasanen A (2009) The application of ground penetrating radar to the study of Quaternary depositional environments. Res Terrae Ser A 27:1–45

Place J, Malehmir A, Högdahl K, Juhlin C, Nilsson KP (2015) Seismic characterization of the Grängesberg iron deposit and its mining-induced structures, central Sweden. Interpretation 3:SY41–SY56. doi:10.1190/INT-2014-0212.1

Pugin AJM, Larson T, Bergler S, McBride J, Bexfield C (2004a) Near-surface mapping using SH-wave and P-wave seismic land-streamer data acquisition in Illinois, U.S. Lead Edge 23:677–682. doi:10.1190/1.1776740

Pugin AJM, Larson T, Sargent S (2004b) 3.5 Km/Day of high resolution seismic reflection data using a landstreamer. In: Symposium on the application of geophysics to engineering and environmental problems 2004. Environment and Engineering Geophysical Society, Denver, CO, pp 1380–1388

Pugin AJM, Pullan S, Hunter J, Oldenborger G (2009a) Hydrogeological prospecting using P- and S-wave landstreamer seismic reflection methods. Surf Geophys. doi:10.3997/1873-0604.2009033

Pugin AJ-M, Pullan SE, Hunter JA (2009b) Multicomponent high-resolution seismic reflection profiling. Lead Edge 28:1248–1261

Pugin AJ, Mäkinen J, Ahokangas E, Artimo A, Vanhala H, Pasanen A, Moisio K, Virtasalo J, Tuusjärvi M (2014) High-resolution seismic reflection survey with landstreamer on the characterization of the Virttaankangas aquifer, SW Finland. In: Virtasalo J, Tuusjärvi M (eds) Abstract book. Guide 58, 1st Finnish National Colloqvium of Geosciences, Espoo, 19–20 March 2014, Geological Survey of Finland, Espoo, pp 63–64

Pullan SE, Pugin AJM, Dyke LD, Hunter JA, Pilon JA, Todd BJ, Allen VS, Barnett PJ (1994) Shallow geophysics in a hydrogeological investigation of the Oak Ridges Moraine, Ontario. In: Proceedings of the Symposium on the Application of Geophysics to Engineering and Environmental Problems: SAGEEP'94, Boston, MA, March 1994, pp 27–31

Punkari M (1980) The ice lobes of the Scandinavian ice sheet during the deglaciation in Finland. Boreas 9:307–310. doi:10.1111/j.1502-3885.1980.tb00710.x

Rossi PM, Ala-aho P, Doherty J, Kløve B (2014) Impact of peatland drainage and restoration on esker groundwater resources: modeling future scenarios for management. Hydrogeol J 22:1131–1145. doi:10.1007/s10040-014-1127-z

Röthlisberger H (1972) Water pressure in intra- and subglacial channels. J Glaciol 11:177–203

Rubin Y, Mavko G, Harris J (1992) Mapping permeability in heterogeneous aquifers using hydrologic and seismic data. Water Resour Res 28:1809–1816. doi:10.1029/92WR00154

Salas-Romero S, Malehmir A, Snowball I, Lougheed BC, Hellqvist M (2016) Identifying landslide preconditions in Swedish quick clays: insights from integration of surface geophysical, core sample- and downhole property measurements. Landslides 13:905–923. doi:10.1007/s10346-015-0633-y

Schmelzbach C, Green AG, Horstmeyer H (2005) Ultra-shallow seismic reflection imaging in a region characterized by high source-generated noise. Surf Geophys 3:33–46. doi:10.3997/1873-0604.2004027

Sharpe DR, Pugin A, Pullan SE, Gorrell G (2003) Application of seismic stratigraphy and sedimentology to regional hydrogeological investigations: an example from Oak Ridges Moraine, southern Ontario, Canada. Can Geotech J 40:711–730. doi:10.1139/t03-020

Sheriff RE, Geldart LP (1995) Exploration seismology. Cambridge University Press, New York

Shreve RL (1985) Esker characteristics in terms of glacier physics, Katahdin esker system, Maine. Geol Soc Am Bull 96:639. doi:10.1130/0016-7606(1985)96<639:ECITOG>2.0.CO;2

Sloan SD, Tsoflias GP, Steeples DW, Vincent PD (2007) High-resolution ultra-shallow subsurface imaging by integrating near-surface seismic reflection and ground-penetrating radar data in the depth domain. J Appl Geophys 62:281–286. doi:10.1016/j.jappgeo.2007.01.001

Steeples D, Miller R (1998) Avoiding pitfalls in shallow seismic reflection surveys. Geophysics 63:1213–1224. doi:10.1190/1.1444422

Steeples DW, Miller RD (1988) Seismic reflection methods applied to engineering, environmental, and groundwater problems. In: Proc. (1st) Symp. on the application of geophysics to engineering and environmental problems, Soc. Eng. and Mineral Exploration Geophysicists, Golden, CO, pp 409–461

Telford WM, Geldart LP, Sheriff RE (1990) Applied geophysics. Cambridge University Press, Cambridge, UK

Theakstone WH (1976) Glacial lake sedimentation, Austerdalsisen, Norway. Sedimentology 23:671–688. doi:10.1111/j.1365-3091.1976.tb00101.x

Tryggvason A, Rögnvaldsson S ður T, Flóvenz ÓG (2002) Three-dimensional imaging of the P- and S-wave velocity structure and earthquake locations beneath southwest Iceland. Geophys J Int 151: 848–866. doi:10.1046/j.1365-246X.2002.01812.x

Ulusoy İ, Dahlin T, Bergman B (2015) Time-lapse electrical resistivity tomography of a water infiltration test on Johannishus Esker, Sweden. Hydrogeol J 23:551–566. doi:10.1007/s10040-014-1221-2

Valjus T (2006) Turun Seudun Vesi. Pohjavesialueen kallionpinnan tason 1073 määritys painovoimamittausten avulla [Turku Region Water Ltd. The determination of the groundwater area's bedrock surface level by gravity measurements]. Geological Survey of Finland, Espoo, pp 41

van der Veen M, Spitzer R, Green A, Wild P (2001) Design and application of a towed land-streamer system for cost-effective 2-D and pseudo-3-D shallow seismic data acquisition. Geophysics 66:482–500. doi:10.1190/1.1444939

van der Veen M, Green AG (1998) Land streamer for shallow seismic data acquisition: evaluation of gimbal-mounted geophones. Geophysics 63:1408–1413. doi:10.1190/1.1444442

Warren WP, Ashley GM (1994) Origins of the ice-contact stratified ridges (eskers) of Ireland. SEPM J Sediment Res. doi:10.1306/D4267DD9-2B26-11D7-8648000102C1865D